Analysis and validation of the potential of the MYO1E gene in pancreatic adenocarcinoma based on a bioinformatics approach

SONGBAI LIU[1*], PENG LIU[1,2*], XIAOBIN FEI[1*], CHANGHAO ZHU[3], JUNYI HOU[1], XING WANG[1,3] and YAOZHEN PAN[1,3]

[1]School of Clinical Medicine, Guizhou Medical University; [2]Department of Hepatobiliary Surgery, The Affiliated Hospital of Guizhou Medical University; [3]Department of Hepatobiliary Surgery, The Affiliated Cancer Hospital of Guizhou Medical University, Guiyang, Guizhou 550000, P.R. China

Received January 23, 2023; Accepted March 22, 2023

DOI: 10.3892/ol.2023.13871

Abstract. Pancreatic adenocarcinoma (PAAD) is a common digestive cancer, and its prognosis is poor. Myosin 1E (MYO1E) is a class I myosin family member whose expression and function have not been reported in PAAD. In the present study, bioinformatics analysis was used to explore the expression levels of MYO1E in PAAD and its prognostic value, and the immunological role of MYO1E in PAAD was analyzed. The study revealed that a variety of malignancies have substantially increased MYO1E expression. Further investigation demonstrated that PAAD tissues exhibited greater levels of MYO1E mRNA and protein expression than normal tissues. High MYO1E expression is associated with poor prognosis in patients with PAAD. MYO1E expression was also associated with pathological stage in patients with PAAD. Functional enrichment analysis demonstrated that MYO1E was linked to multiple tumor-related mechanisms in PAAD. The pancreatic adenocarcinoma tumor microenvironment (TME) was analyzed and it was revealed that MYO1E expression was positively associated with tumor immune cell infiltration. In addition, MYO1E was closely associated with some tumor chemokines/receptors and immune checkpoints. *In vitro* experiments revealed that the suppression of MYO1E expression could inhibit pancreatic adenocarcinoma cell proliferation, invasion and migration. Through preliminary analysis, the present study evaluated the potential function of MYO1E in PAAD and its function in TME, and MYO1E may become a potential biomarker for PAAD.

Correspondence to: Professor Yaozhen Pan or Dr Xing Wang, School of Clinical Medicine, Guizhou Medical University, 9 Beijing Road, Yunyan, Guiyang, Guizhou 550000, P.R. China
E-mail: panyaozhen@gmc.edu.cn
E-mail: foxmulder180@gmc.edu.cn

*Contributed equally

Key words: myosin 1E, pancreatic adenocarcinoma, bioinformatics, tumor microenvironment, immune cell infiltration

Introduction

PAAD is among the deadliest malignant tumors of the digestive system, with a high rate of recurrence, a high fatality rate, and a poor prognosis (1). In the early stages, there are few characteristic clinical signs and no reliable screening tools; up to 85% of patients with PAAD are diagnosed at advanced stages or develop distant metastases (2), and it is the seventh leading cause of cancer death (3). Despite ongoing advances in therapy, PAAD is still one of the most difficult cancers to treat, with a 5-year survival rate of less than 10% (4). The incidence of PAAD is projected to rise to 18.6‰ in 2050, with an average yearly increase of 1.1% (5). Therefore, the underlying mechanisms of PAAD should be thoroughly investigated, and the search for potential therapeutic targets becomes crucial.

Myosins are classifiable into 24 classes based on the amino acid sequence of the ATP hydrolytic region, and they are involved in various cellular functions, including organelle transport, actin recombination, and cell signal transduction (6). Class I myosin consists of Myo1a~Myo1h (7), an actin-dependent molecular motor expressed in various organisms, from yeast to humans (8). Class I myosins may interact with actin filaments and cell membranes through their N-terminal motor structural domain and C-terminal tail homology 1 (TH1) structural domain, respectively; in addition to the TH1 structural domain, class I myosins also include the proline-rich TH2 structural domain and the SH3 structural domain (9,10). According to previous research, MYO1E contributes to the progression of breast cancer and affects breast tumor cell differentiation and proliferation (11). The role of MYO1E in PAAD has yet to be reported, and its related mechanisms still need further investigation.

In this research, we found that MYO1E was substantially expressed in PAAD and negatively correlated with PAAD patient survival prognosis. Functional and pathway enrichment analyses revealed that MYO1E was linked to tumor-associated pathways. In addition, MYO1E was involved in multiple tumor immune cell infiltrates in the TME. Further validation of the impact of MYO1E on the proliferation, invasion, and migration of PAAD cells was provided by *in vitro* tests. Our results reveal the clinical significance, potential function, and immune relevance of

MYO1E in PAAD, which may provide new strategies for the early diagnosis and prognosis of PAAD. The study flowchart is shown in Fig. 1.

Materials and methods

MYO1E gene expression analysis. We used RNAseq data in FPKM format from The Cancer Genome Atlas Project (12) (TCGA) (https://portal.gdc.cancer.gov/, Version 35) and Genotype-Tissue Expression (13) (GTEx) (https://www.gtexportal.org/, Version 8) processed uniformly by the UCSC XENA (University Of California Sisha Cruz, https://xenabrowser.net/datapages/, July 20, 2019) database to extract the TCGA corresponding to 33 tumors data and normal tissue data in GTEx. The calculation was performed using the 'stats' package in R (Version 4.2.1) (https://cran.r-project.org/), the Wilcoxon rank sum test was used, and the results were visualized using the 'ggplot2' package. The CPTAC module of the UALCAN database (http://ualcan.path.uab.edu/, May 13, 2022) analyzed the total protein expression of MYO1E in different cancers. Finally, we compared MYO1E expression in PAAD tissues and normal tissues in the GEO (GSE16515, GSE62165, and GSE15471) cohort (https://www.ncbi.nlm.nih.gov/geo/).

Tissue samples. Fifteen cases of pancreatic adenocarcinoma and matched adjacent normal tissues were obtained from the Affiliated Hospital of Guizhou Medical University and the Cancer Hospital Affiliated with Guizhou Medical University. Patients were informed and signed an informed consent form agreeing to use their tissues for scientific research. This study was approved by the ethics committees of the Affiliated Hospital of Guizhou Medical University and the Cancer Hospital Affiliated with Guizhou Medical University. All specimens were frozen and stored at -80˚C before western blot and reverse transcription-quantitative polymerase chain reaction (RT-qPCR) analysis.

Survival analysis. GEPIA2 (http://gepia2.cancer-pku.cn/, Version 2) is a platform for gene expression analysis based on tumor and normal samples from TCGA and GTEx databases (14). We obtained the overall survival (OS) and disease free survival (DFS) of the MYO1E gene in PAAD using the 'Survival analysis' panel of the GEPIA2 database with a 95% confidence interval.

Univariate and multifactorial regression analysis. RNAseq data and corresponding clinical information for pancreatic adenocarcinoma were obtained from TCGA dataset (TCGA-PAAD, Version 35). The influence of MYO1E and clinical features of PAAD patients (age, gender, M-stage, pTNM-stage, and grading) on 'OS' was evaluated using univariate and multivariate regression models (P<0.05) using the 'forestplot' package. Following this analysis's findings, we created a Nomogram using the 'rms' package to forecast the overall recurrence rate at 1, 2, and 3 years. Using the 'stage plot' panel of GEPIA2, the link between MYO1E and the pathological stage of PAAD was assessed. P<0.05 was considered significant.

Differentially expressed genes analysis. In the TCGA database, the median expression of MYO1E was separated between high and low expression groups, and 237 differential genes were obtained and analyzed for differential expression using the 'Limma' package of R. Differentially expressed genes (DEGs) were considered as the threshold value with log2 (fold change) >1 and adjusted P<0.05.

String protein network analysis. We built a protein-protein interaction network (PPI) of MYO1E-binding proteins through the STRING website (http://STRING-DB.org/); using the main settings 'evidence', 'experimental', and 'low confidence', the top 50 MYO1E-interacting proteins were obtained. Next, using the 'similar genes detection' module of GEPIA2, the top 100 target genes connected with MYO1E were selected. We used an interactive Venn diagram viewer (Jvenn) (15) to intersect the two sets of data.

Enrichment analysis. We used R's 'clusterProfiler', 'enrichplot', and 'org.Hs.eg.db' packages for Gene Ontology (GO) and Kyoto Encyclopedia of Genes and Genomes (KEGG) enrichment analysis and 'ggplot2' for bubble and histogram plots. P<0.05 is considered to be a meaningful pathway.

Immunological characterization. We downloaded RNAseq data from the TCGA database for PAAD. We used the TIMER algorithm for the immune scoring of B cells, $CD4^+$ T cells, $CD8^+$ T cells, neutrophils, macrophages, and myeloid dendritic cells via the 'immunedeconv' package. We continued to explore the expression and infiltration of MYO1E in these cells using the 'immunegene' module in the TIMER2.0 database (https://cistrome.shinyapps.io/Timer/) (16). Immunoinfiltration of tumor-associated fibroblasts was assessed by the MCPCOUNTER and EPIC algorithms. In addition, TISIDB (http://cis.hku.hk/TISIDB/) is a database that can query the immune interactions of specific genes with tumors (17), and we evaluated the relationship between MYO1E and chemokines/receptors through the 'chemokine' module. Finally, we extracted the expression of CD274, CTLA4, HAVCR2, LAG3, PDCD1, PDCD1LG2, TIGIT, and SIGLEC15 and analyzed the expression of MYO1E and immune checkpoints by 'pheatmap' package. Adjusted P<0.05 was considered significant.

Cell culture and transfection. Human normal pancreatic ductal epithelial cells (HPDE) from Cellosaurus cell bank (https://www.cellosaurus.org/) and pancreatic adenocarcinoma cell lines (ASPC-1, BxPC-3, MIA PaCa-2, and PANC-1) were obtained from the Chinese Academy of Sciences (https://www.cellbank.org.cn/). HPDE, ASPC-1, and BxPC-3 cells were cultured in RPMI1640 (Gibco) containing 10% fetal bovine serum and 1% P/S; MIA PaCa-2 and PANC-1 cells were cultured in DMEM under the same conditions, and all cells were cultured at 37˚C in a 5% CO_2 incubator. The si-MYO1E target sequence was si-MYO1E#1 (sense 5'-CAGAAGCAACUACCUCUGAAA-3'; antisense 5'-UUUCAGAGGUAGUUGCUUCUG-3'), si-MYO1E#2 (sense 5'-CCUCAUAGAGAACAAAGUGAA-3'; antisense 5'-UUCACUUUGUUCUCUAUGAGG-3') (Sangon Biotech) were transfected using Lipofectamine 3000 (Invitrogen; Thermo Fisher Scientific), and all steps were performed strictly according to the instructions.

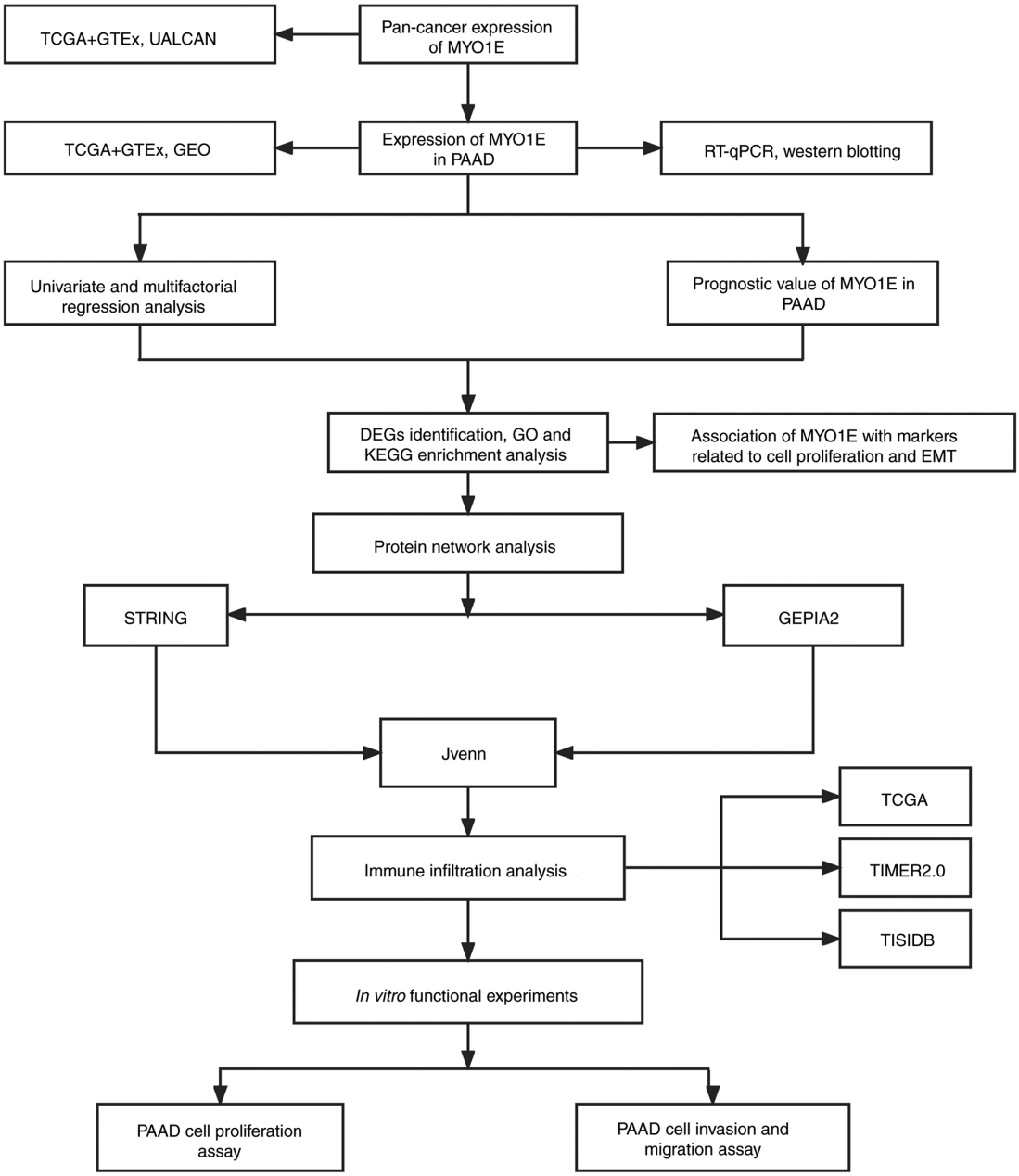

Figure 1. Flowchart of the study design. DEGs, differentially expressed genes; EMT, epithelial-mesenchymal transition; GEO, Gene Expression Omnibus; GEPIA2, Gene Expression Profiling Interactive Analysis 2; GO, Gene Ontology; GTEx, Genotype-Tissue Expression; KEGG, Kyoto Encyclopedia of Genes and Genomes; MYO1E, myosin 1E; PAAD, pancreatic adenocarcinoma; RT-qPCR, reverse transcription-quantitative PCR; STRING, Search Tool for the Retrieval of Interacting Genes/Proteins; TCGA, The Cancer Genome Atlas; TIMER2.0, Tumor Immune Estimation Resource 2.0; UALCAN, The University of Alabama at Birmingham Cancer Data Analysis Portal.

Reverse transcription-quantitative PCR (RT-qPCR) assay. PAAD tissues or cell lines were treated with TRIzol (Invitrogen; Thermo Fisher Scientific) to extract total RNA. RNA quality and concentration were determined using a NanoDrop spectrophotometer (Thermo Fisher Scientific), and reverse transcription was performed using the PrimeScript™ RT Reagent kit (Takara). RT-qPCR analysis was performed using TB Green® Premix Ex Taq TM (Takara). The MYO1E primer sequence was sense 5'-GCAGCAGTCTACCAGTTC-3' and antisense 5'-GAG CGTCATAGGCATACAA-3'. GAPDH (sense 5'-CCACAG TCCATGCCATCACTG-3'; antisense 5'-GTCAGGTCCACC ACTGACACG-3') was selected as the endogenous reference. The $2^{-\Delta\Delta Cq}$ method (18) was used to calculate the experimental results.

Western blot assay. Total proteins from PAAD tissues or cell lines were extracted using radio immunoprecipitation assay (RIPA) lysate (Merck Millipore), and protein quantification was performed using the BCA kit. Then, 5x loading buffer was added and boiled for 10 min at 95˚C. The proteins were separated by electrophoresis using 10% sodium dodecyl sulfate-polyacrylamide gel (SDS-PAGE) and then transferred to a 0.45 μm PVDF membrane. Five percent skim milk was blocked at room temperature for 2 h, incubated with the corresponding primary antibodies MYO1E, Cyclin E2, GAPDH,

CDK4, CDK2, P27, E-cadherin, vimentin, N-cadherin (all the above antibodies were from Proteintech, China) overnight at 4˚C. TBST was washed 3 times and incubated with the corresponding species; secondary antibodies were incubated at room temperature for 2 h, and ECL reagent (Boster) was used for exposure imaging.

Cell proliferation, migration and invasion assays. CCK-8 experiment: CCK-8 chromogenic solution (GlpBio) was added to 96-well plates containing $3x10^3$ cells per well and incubated for 2 h at 37˚C, and absorbance values at 450 nm were measured.

EDU incorporation experiment. Using the Click-iT EDU-555 kit (Servicebio), 20 μM EDU storage solution was added and incubated for 2 h, and the fluorescent dye iF555 was used for staining. Photographs were taken under a fluorescence microscope (Nikon Japan).

Wound healing assay. When cell fusion in the 6-well plate reached 100%, the cells were scratched using the tip of a 200 μl pipette, and the wound area was recorded after 0 h, 24 h, and 48 h incubation in serum-free medium.

Cell migration assay. In an upper chamber of a Transwell plate containing 200 μl of serum-free media (NEST Biotechnology Co.), $1x10^4$ cells were seeded, and 800 μl of medium containing 20% fetal bovine serum was added to the bottom chamber. Migrating cells were stained with 0.5% crystal violet. The same method was used for cell invasion experiments, except that matrix gel was added at a concentration of 50 mg/l in the upper chamber of the Transwell plate (R&D Systems).

Statistical analysis. Pan-cancer comparative analysis was performed using the Mann-Whitney U test. A paired Student's t-test was used to compare the RT-qPCR data for the collected pancreatic adenocarcinoma tissues and their adjacent normal tissues. For datasets containing multiple groups, one-way ANOVA with Tukey and least significant difference post hoc multiple comparison tests was used. Survival analysis was performed using the Kaplan-Meier method and log-rank test. The impact of MYO1E and clinical features of PAAD on OS was analyzed using univariate and multifactorial regression, and nomograms were constructed to predict the OS of PAAD at 1, 2, and 3 years. The association between MYO1E and tumor pathways was evaluated using Spearman's correlation coefficients. All statistical analyses were performed using R. The statistical threshold is $P<0.05$, and continuous data were reported as the mean ± standard deviation.

Results

Expression analysis of MYO1E in different cancers. To explore the expression of MYO1E in different cancers, we analyzed the expression level of MYO1E in 33 malignancies using the TCGA and GTEx datasets. The findings demonstrated that MYO1E expression kurtosis was elevated in tumor tissues relative to normal tissues in the vast majority of malignancies, including PAAD (Fig. 2A). Next, we used CPTAC to assess the levels of MYO1E protein expression in each tumor. The findings indicated that MYO1E expression was higher in lung adenocarcinoma (LUAD), glioblastoma (GBM), PAAD, colon adenocarcinoma (COAD), breast invasive carcinoma (BRCA), and head and neck squamous carcinoma (HNSC) than in normal tissues (Fig. 2B). Combining the data of each database, we found that the elevated expression of MYO1E in PAAD was more stable; thus, we further investigated the specific role of MYO1E in PAAD.

Expression of MYO1E in PAAD. Based on the above screening results, to verify the expression of MYO1E in PAAD, we collected three datasets (GSE16515, GES62165, and GSE15471) through the GEO database. We found that MYO1E expression was considerably greater in PAAD tissues than in normal tissues (Fig. 3A). We verified this by RT-qPCR and western blotting experiments using collected PAAD tissues and paired adjacent normal tissues. We found that the mRNA and protein expression levels of MYO1E in PAAD tissues were higher than those in normal tissues (Fig. 3B and C). Next, we used RT-qPCR and a Western blot assay to measure the amount of MYO1E expression in PAAD cell lines. The findings revealed that MYO1E was substantially expressed in PAAD cell lines (Fig. 3D). In addition, the immunofluorescence colocalization assay showed that MYO1E was localized in the cytoplasm (Fig. 3E).

Clinical prognostic correlation between MYO1E and PAAD. MYO1E is abundantly expressed in PAAD tissues, so we wanted to analyze the relationship between MYO1E and PAAD patients. We downloaded the RNAseq data and clinical information of PAAD patients from the TCGA database. Through univariate and multivariate regression analyses, MYO1E might function as a standalone prognostic factor for PAAD (Fig. 4A and B). The nomogram further indicated that MYO1E could be used as an independent factor affecting PAAD patients' OS and predict the prognosis at 1, 2, and 3 years (Fig. 4C and D). To clarify the connection between MYO1E and PAAD survival prognosis, we demonstrated by Kaplan-Meier analysis that high MYO1E expression was inversely connected with OS and DFS in PAAD patients (Fig. 4E). In addition, the GEPIA2 database also found that MYO1E was associated with the pathological stage of PAAD (Fig. 4F). These data indicated that MYO1E might have a cancer-promoting function in PAAD.

Potential function of MYO1E in PAAD. To analyze the potential biological functions of MYO1E in PAAD, we performed enrichment analysis by DEGs. We downloaded the RNAseq data and clinical information of PAAD patients from TCGA database. Patients were into high and low expression groups based on the median expression of MYO1E in PAAD. The two groups of DEGs were compared using $|log2FC|>1$. We found 237 genes with differential expression, including 236 upregulated genes and 1 downregulated gene (Fig. 5A). The heatmap (Fig. 5B) shows the expression of these DEGs in different tissues. As there is only one downregulated gene, it is not being analyzed. Then, we performed KEGG and GO enrichment analyses on the upregulated DEGs. The findings

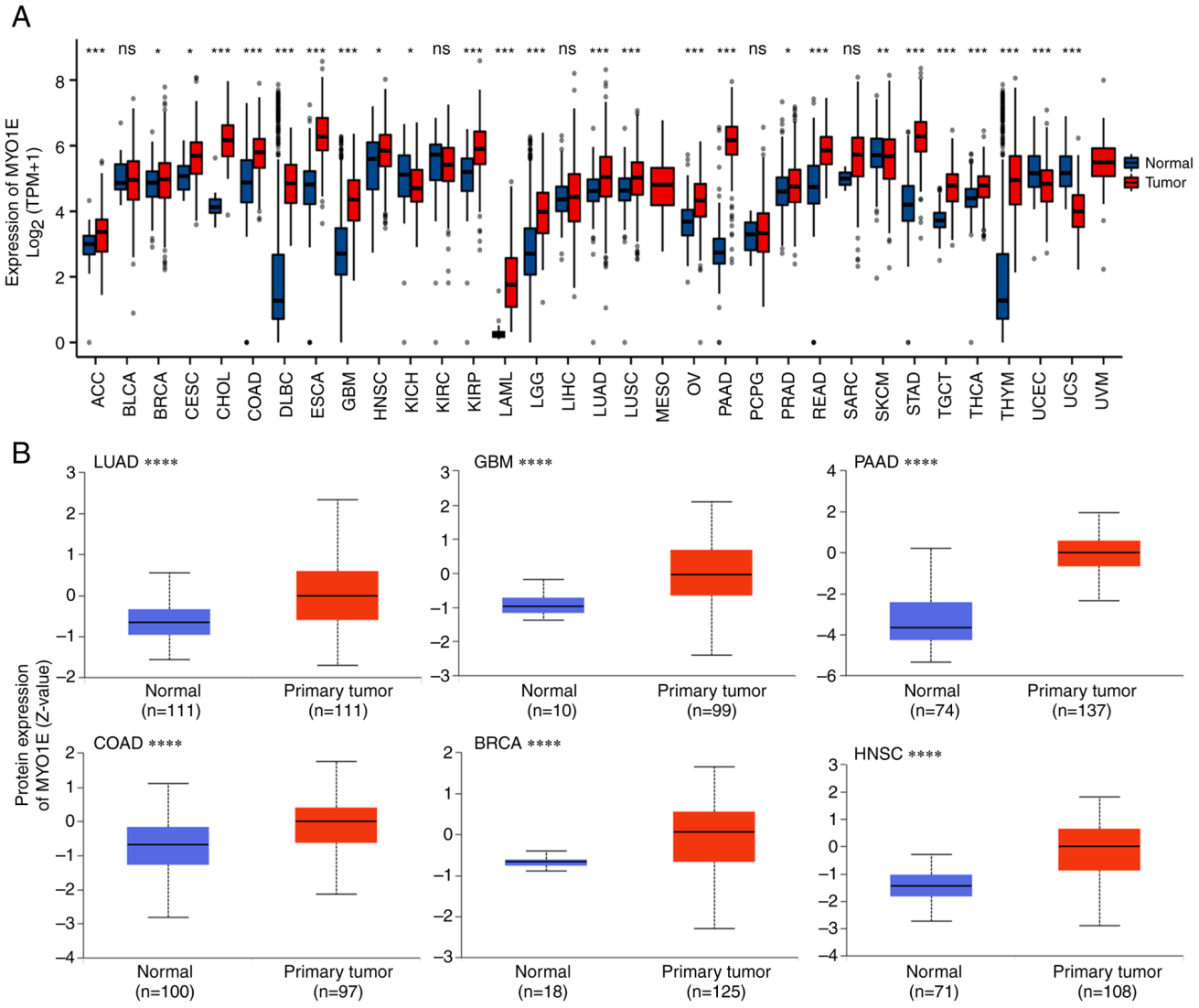

Figure 2. Expression levels of MYO1E in different tumor tissues and normal tissues. (A) Analysis of MYO1E expression in 33 tumors based on TCGA (version 35) and GTEx (version 8) data using R (version 4.2.1). In some cases, statistical analysis could not be performed because only tumor tissue data but not normal tissue data were provided. (B) Based on Clinical Proteomic Tumor Analysis Consortium and the International Cancer Proteogenome Consortium data, using UALCAN (May 13, 2022) database analysis of MYO1E protein expression in LUAD, GBM, PAAD, COAD, BRCA and HNSC. *P<0.05, **P<0.01, ***P<0.001, ****P<0.0001. The normal tissues shown in (A) include unpaired healthy control tissues from TCGA and GTEx; The normal tissues in (B) are from the Clinical Proteomic Tumor Analysis Consortium and the International Cancer Proteogenome Consortium datasets in the UALCAN database. BRCA, breast invasive carcinoma; COAD, colon adenocarcinoma; GBM, glioblastoma; GTEx, Genotype-Tissue Expression; HNSC, head and neck squamous carcinoma; LUAD, lung adenocarcinoma; MYO1E, myosin 1E; ns, not significant; PAAD, pancreatic adenocarcinoma; TCGA, The Cancer Genome Atlas; TPM, transcripts per million.

of the KEGG enrichment analysis demonstrated that upregulated DEGs were mostly related to the PI3K-AKT signaling pathway, ECM-receptor interaction, and proteoglycans (Fig. 5C). In addition, the GO enrichment analysis showed that upregulated DEGs were associated with extracellular structural organization, extracellular matrix organization, epithelial cell proliferation, and cell-substrate adhesion (Fig. 5D). So we analyzed the markers related to MYO1E and cell proliferation and migration through the TCGA database. The results showed that MYO1E was positively correlated with CDK2, CDK4, CDK6, CCNB1 (Cyclin B1), CCND1 (Cyclin D1), CCNE2 (Cyclin E2), FN1, SNAIL, and VIM (Vimentin) (Fig. 6A-C). These results indicated that MYO1E might regulate cell proliferation and Epithelial-Mesenchymal Transition (EMT).

Molecular interactions of MYO1E in PAAD. To further investigate the intrinsic mechanism of MYO1E gene in tumorigenesis, we screened the top 50 proteins bound to MYO1E using the STRING database (Fig. 7A) and identified the top 100 genes related to MYO1E expression in PAAD utilizing the GEPIA2 database. Cross-tabulation examination of the two datasets above revealed that ARPC5 and ARPC2 crossed each other (Fig. 7B). We performed an enrichment analysis on both datasets. The KEGG enrichment analysis indicated that MYO1E might participate in the Ras signaling pathway, phosphatidylinositol signaling system, and Hippo signaling pathway (Fig. 7C). The GO enrichment analysis showed that MYO1E was involved in adhesion, EMT, epithelial cell proliferation, and migration (Fig. 7D). Furthermore, we analyzed ARPC5 and ARPC2 proteins. GEPIA2 database analysis

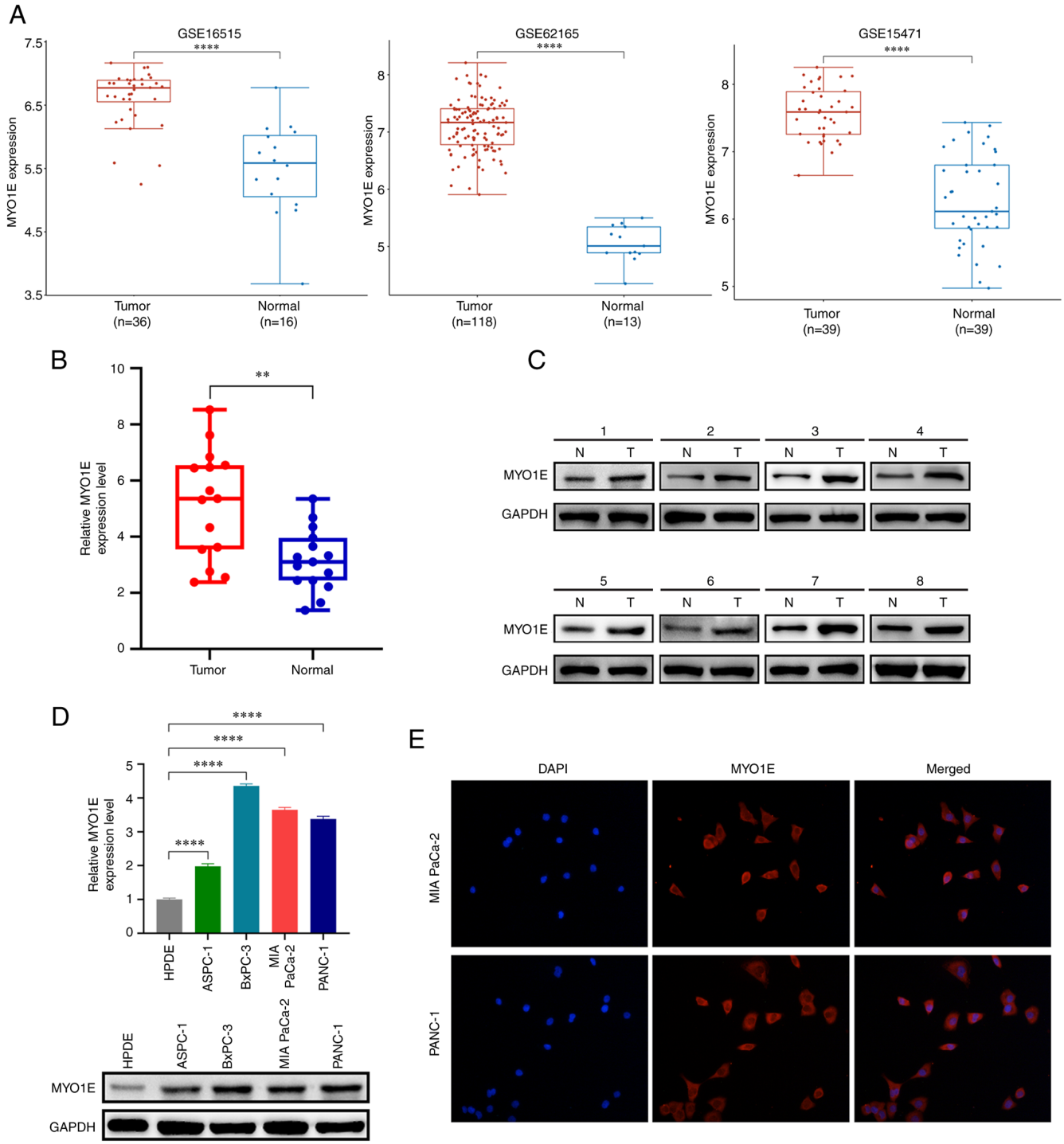

Figure 3. Expression levels of MYO1E in pancreatic adenocarcinoma. (A) MYO1E expression in the GSE16515, GSE62165 and GSE15471 datasets. (B) Analysis of MYO1E expression in our collected PAAD tissues and adjacent normal tissues using RT-qPCR. (C) Analysis of MYO1E expression in our collected PAAD tissues and adjacent normal tissues using western blotting. (D) RT-qPCR and western blot analyses of MYO1E expression in PAAD cell lines (Tukey post hoc test). (E) Immunofluorescence co-localization showed that MYO1E was localized in the cytoplasm. Magnification, x200. **P<0.01, ****P<0.0001. MYO1E, myosin 1E; PAAD, pancreatic adenocarcinoma; RT-qPCR, reverse transcription-quantitative PCR; N, normal tissue; T, tumor tissue.

revealed that ARPC5 and ARPC2 are also highly expressed in PAAD (Fig. 7E and F). ARPC5 and ARPC2 are members of the actin-related protein 2/3 complex (Arp2/3) (19,20) and are involved in tumor development. Examples include multiple myeloma (21), breast cancer (22), and gastric cancer (23). Notably, related literature reported the analysis of ARPC5 and ARPC2 in immunology, suggesting that ARPC5 and ARPC2 may be crucial for tumor immunity (24-26).

Relationship between MYO1E expression and immune characteristics. MYO1E is a potential interacting protein of ARPC5 and ARPC2, and we next investigated MYO1E in immunological aspects. As a major component of the TME, tumor-infiltrating immune cells are essential for tumor growth (27,28). Using the TIMER method, we evaluated the connection between MYO1E and immune cell infiltration with the 'immunedeconv' package. We found that

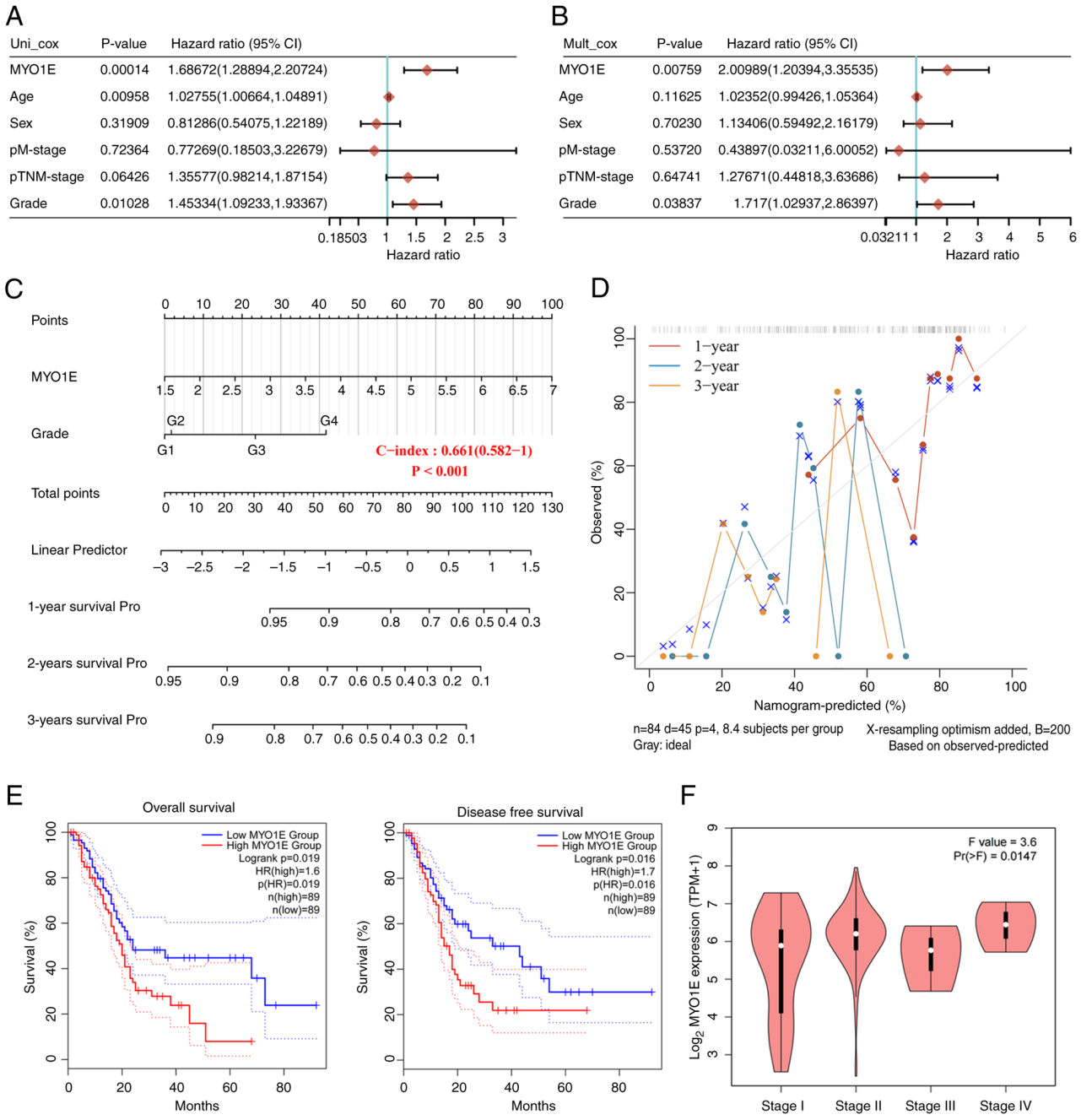

Figure 4. Association between MYO1E expression and pancreatic adenocarcinoma survival prognosis. (A-D) Based on TCGA (version 35) data, the association between MYO1E and survival and prognosis of patients with PAAD was analyzed. (A) Univariate and (B) multifactorial regression analyses of the interaction between MYO1E and clinical features of PAAD. (C) A nomogram of MYO1E and grade was established to predict 1-, 2- and 3-year survival rates of patients with PAAD. (D) OS of patients with PAAD at 1, 2 and 3 years was predicted using calibration curves. (E) Based on TCGA and GTEx data, the OS and disease-free survival curves of groups of patients with PAAD based on MYO1E expression were obtained using the GEPIA2 database. (F) GEPIA2 was used to explore the connection between pathological stage and MYO1E (one-way ANOVA with Tukey post hoc test). GEPIA2, Gene Expression Profiling Interactive Analysis 2; GTEx, Genotype-Tissue Expression; HR, hazard ratio; MYO1E, myosin 1E; OS, overall survival; PAAD, pancreatic adenocarcinoma; TCGA, The Cancer Genome Atlas; TPM, transcripts per million; survival Pro, survival probability; p, pathology.

MYO1E was substantially linked to higher B-cell scores, $CD8^+$T cells, neutrophils, macrophages, and dendritic cells (Fig. 8A). Additional investigation found that MYO1E expression was negatively correlated with tumor purity (cor=-0.183, P=1.61e^{-02}) and positively correlated with $CD8^+$T cells (cor=0.376, P=4.03e-07), B cells (cor=0.261 P=5.53e-04), macrophages (cor=0.29, P=1.21e-04), neutrophils (cor=0.437, P=2.33e-09), and dendritic cells (cor=0.475, P=5.46e-11). At the same time, there was no significant relationship with $CD4^+$T. Cancer-associated fibroblasts regulate tumor-infiltrating immune cells (29,30), and we further confirmed whether MYO1E has a relationship with cancer-associated fibroblasts. Using the TIMER2.0 database with MCPCOUNTER and EPIC algorithms, we found that MYO1E was significantly associated with cancer-associated fibroblasts (EPIC: Rho=0.505, P=1.99e^{-12}, MCPCOUNTER: Rho=0.456, P=3.69e^{-10}) (Fig. 8B). Furthermore, chemokines can be expressed by cells, including immune cells and stromal

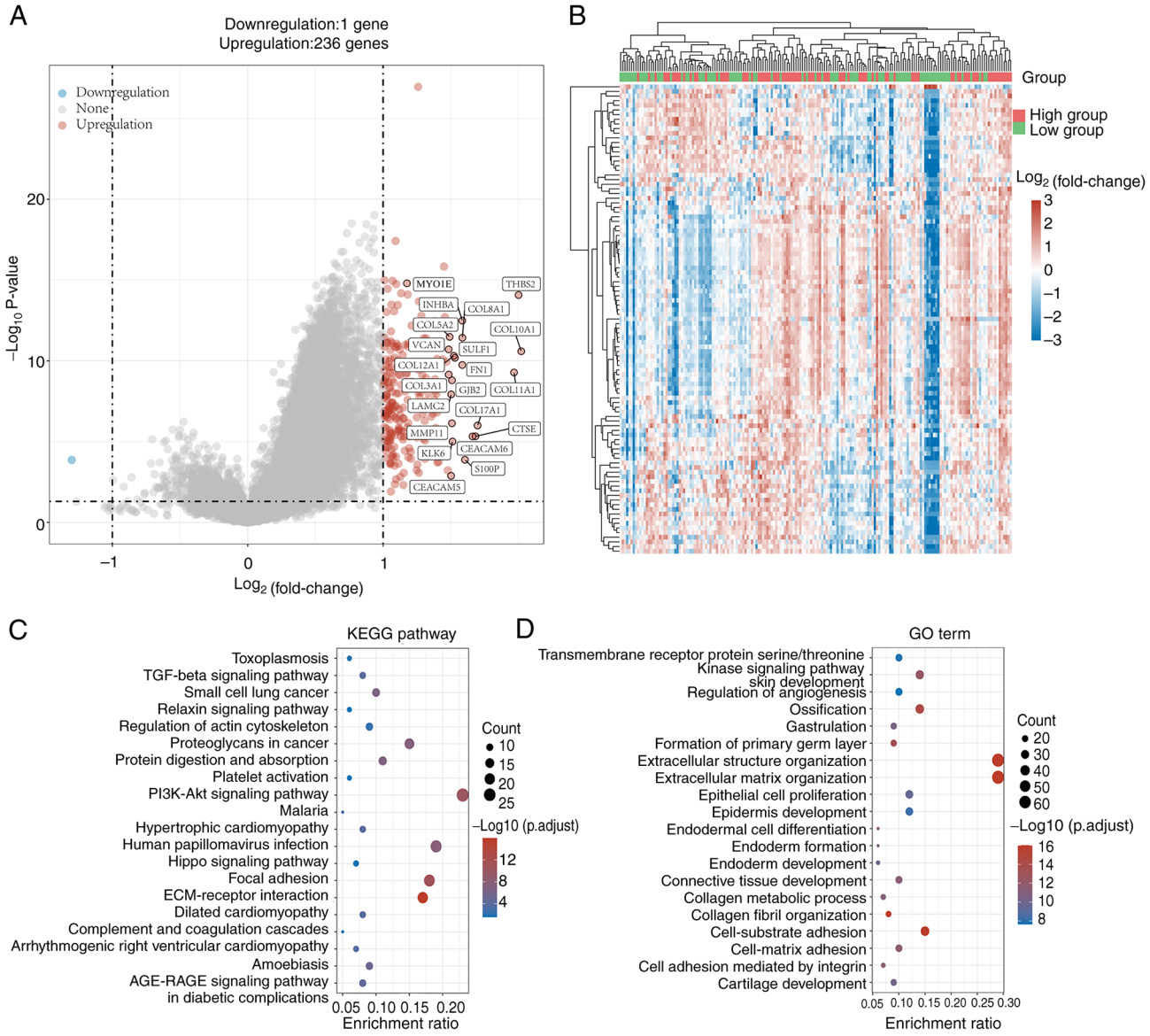

Figure 5. Functional enrichment analysis of DEGs based on The Cancer Genome Atlas (version 35) data. (A) Differences in genes between groups with high and low MYO1E are shown on a volcano map. (B) Heat map analysis of MYO1E expression-related DEGs. (C) KEGG and (D) GO enrichment analysis of upregulated DEGs. DEGs, differentially expressed genes; ECM, extracellular matrix; GO, Gene Ontology; KEGG, Kyoto Encyclopedia of Genes and Genomes; MYO1E, myosin 1E; AGE, advanced glycation end products; RAGE, AGE receptor; p.adjust, adjusted P-value.

cells in TME (31), regulating the phenotype and function of immune cells by modulating their localization and cellular interactions in lymphoid tissue and TME (32). We found that MYO1E was positively correlated with CCL7, CCL24, CXCL14, CCR1, CCR3, and CCR8 through the TISIDB database analysis (Fig. 9A and B), and MYO1E may be implicated in immune cell migration to TME. The primary purpose of immune checkpoint molecules associated with tumor cells is to mediate immune evasion and play a crucial role in maintaining several malignant tendencies (33). Finally, we investigated the expression of high and low MYO1E groups with immune checkpoints. We downloaded RNAseq data and clinical information of PAAD patients from TCGA database and used the 'ggplot2' package for analysis. The results showed that CD274 ($p=9.67e^{-08}$), HAVCR2 ($p=1.39e^{-04}$, PDCD1LG2 ($p=4.26e^{-08}$, and SIGLEC15 ($p=5.00e^{-02}$) were significantly elevated in the high expression group of MYO1E (Fig. 9C).

Silencing of MYO1E inhibits proliferation, invasion and migration of pancreatic adenocarcinoma cells in vitro. Based on the above preliminary bioinformatics analysis, we conducted *in vitro* tests to further confirm the impact of MYO1E on PAAD cells. Through the above validation on PAAD cell lines, we selected MIA PaCa-2 and PANC-1 for experimental studies. We constructed MYO1E small interfering RNA (Si-NC, Si-MYO1E#1, and Si-MYO1E#2) and performed RT-qPCR and Western blotting for validation (Fig. 10A and B). The CCK-8 and EDU incorporation experiment demonstrated that MYO1E downregulation effectively suppressed the proliferation ability of PAAD cells (Fig. 10C-E). We subsequently studied the impact of MYO1E on cyclins, and the Western blot analysis results indicated that downregulation of MYO1E led to reduced expression of Cyclin E2, CDK4, and CDK2 and increased expression of P27 (Fig. 10F). A wound healing test and Transwell assay

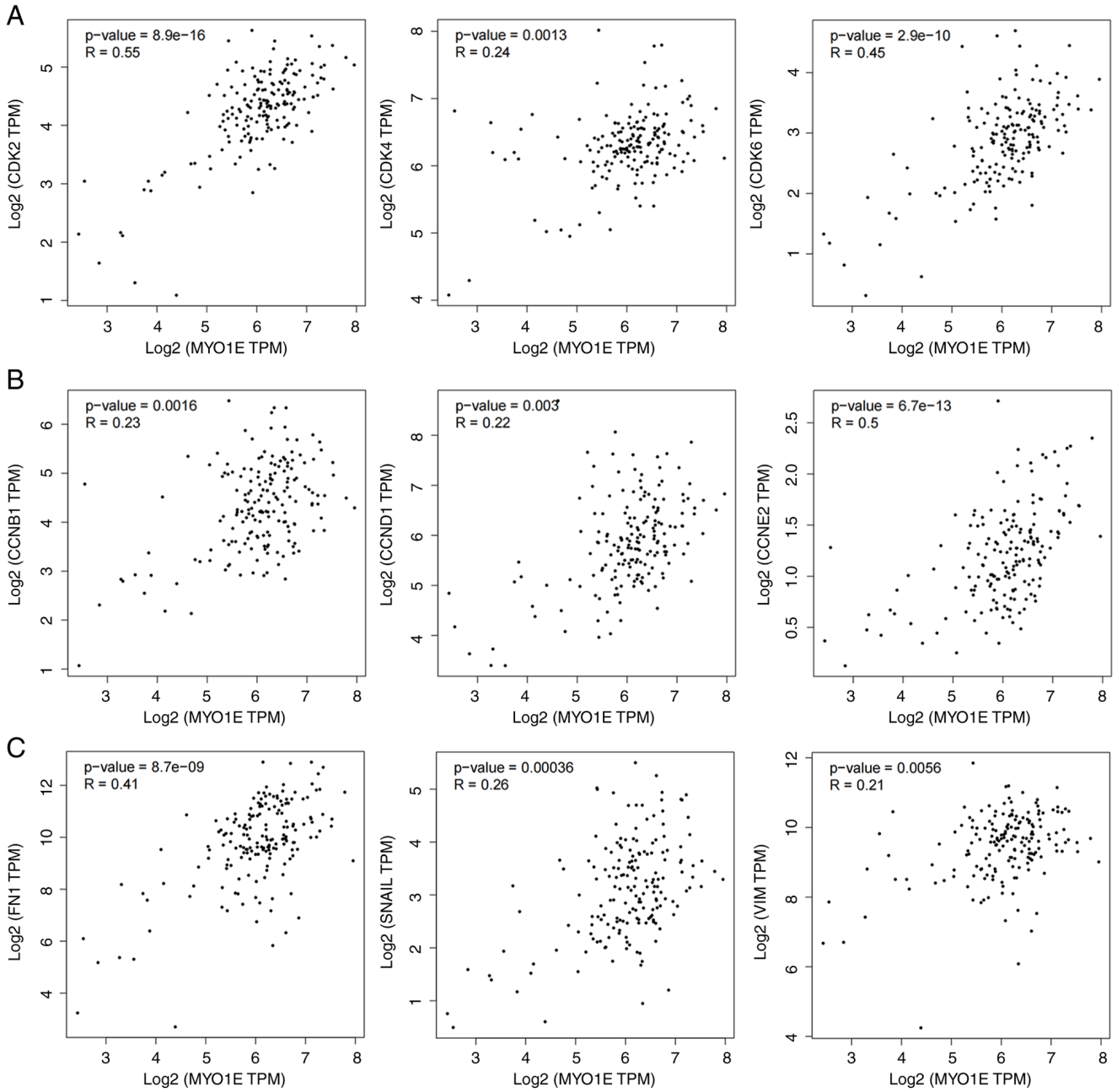

Figure 6. Based on The Cancer Genome Atlas data, scatter plots of MYO1E expression and cell proliferation and EMT marker expression were obtained using the Gene Expression Profiling Interactive Analysis 2 (version 2) database. (A) Relationship between MYO1E and CDK2, CDK4 and CDK6. (B) Relationship between MYO1E and CCNB1, CCND1 and CCNE2. (C) Relationship between MYO1E and FN1, SNAIL and VIM. CCNB1, cyclin B1; CCND1, cyclin D1; CCNE2, cyclin E2; FN1, fibronectin 1; MYO1E, myosin 1E; TPM, transcripts per million; VIM, vimentin.

were conducted to confirm the impact of MYO1E on the invasion and migration of PAAD cells. The wound healing experiment revealed that MYO1E downregulation reduced PAAD cell migration ability (Fig. 11A-D). The Transwell experiment revealed that the number of invading and migrating PAAD cells decreased when MYO1E was down-regulated compared with the control group (Fig. 11E-H). We validated the EMT protein by Western blot assay. The downregulation of MYO1E resulted in decreased expression of N-cadherin and vimentin and increased expression of E-cadherin (Fig. 11I). These findings imply that silencing MYO1E decreases PAAD cell proliferation, invasion, and migration.

Discussion

PAAD is one of the solid tumors with the worst prognosis. American Society of Clinical estimates that there will be approximately 57,600 new cases and 47,050 PAAD deaths in the United States in 2020, with a mortality rate almost similar to the incidence rate and second only to colon cancer among gastrointestinal tumors (34,35). Therefore, early diagnosis and treatment of PAAD are crucial, and the search for efficient biomarkers and fresh treatment targets is crucial.

MYO1E is a member of the class I myosins. Localization studies have shown that MYO1E is present in regions of high actin concentration (36) and can bind ATP and the motor head

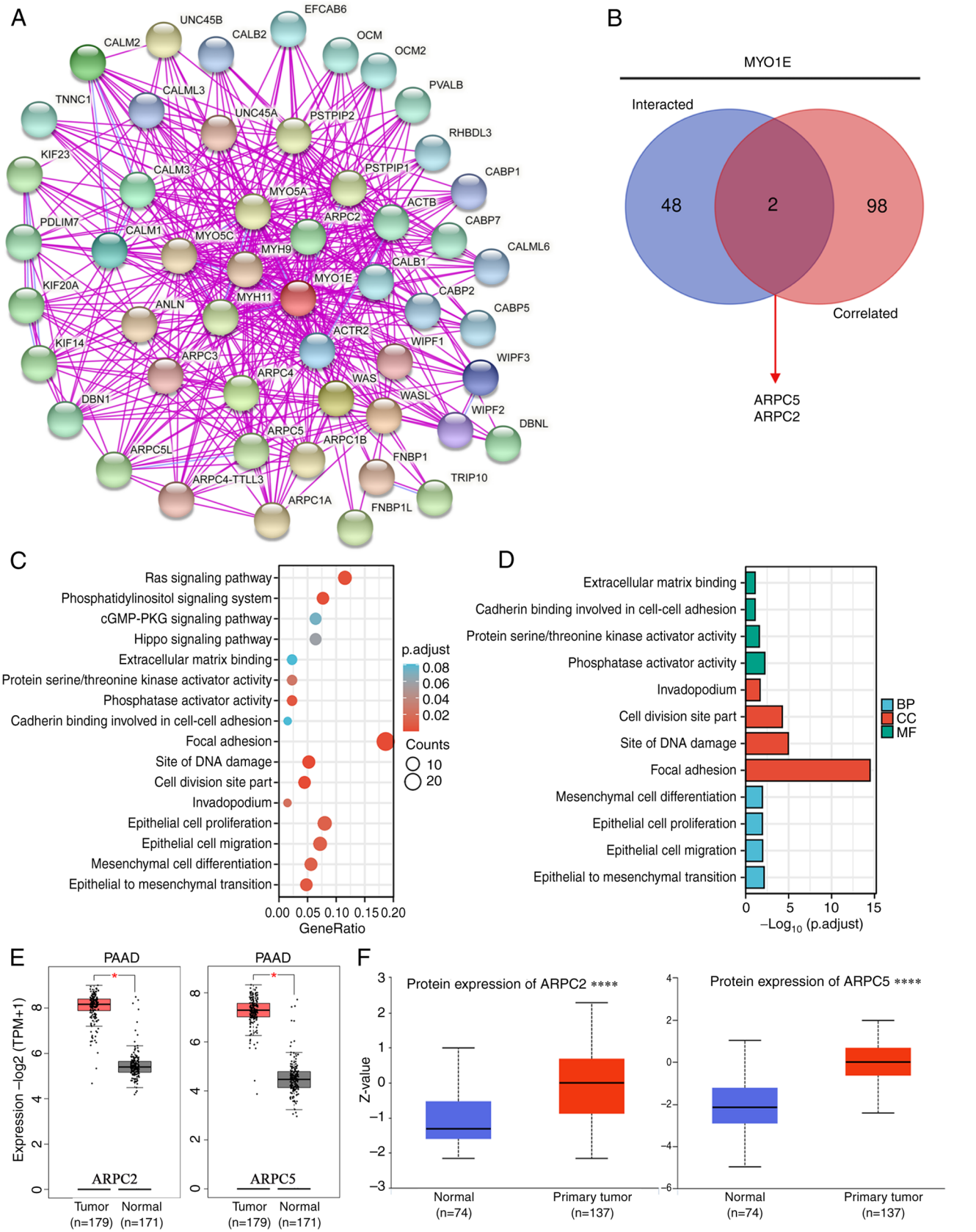

Figure 7. Potential mechanism of MYO1E in PAAD. (A) Top 50 genes interacting with MYO1E were obtained from the STRING database. (B) Venn diagram of the intersection between the top 50 genes interacting with MYO1E and the top 100 genes correlated with MYO1E (as determined using STRING and GEPIA2, respectively). (C) Kyoto Encyclopedia of Genes and Genomes and (D) Gene Ontology enrichment analysis of potential biological processes of MYO1E in PAAD. (E) Boxplots of ARPC5 and ARPC2 mRNA expression were obtained using the GEPIA2 database. (F) Boxplots of ARPC5 and ARPC2 protein expression were obtained using the UALCAN database (May 13, 2022). *P<0.05, ****P<0.0001. ARPC, actin related protein 2/3 complex subunit; BP, biological process; CC, cellular component; GEPIA2, Gene Expression Profiling Interactive Analysis 2; MF, molecular function; MYO1E, myosin 1E; PAAD, pancreatic adenocarcinoma; STRING, Search Tool for the Retrieval of Interacting Genes/Proteins; TPM, transcripts per million; p.adjust, adjusted P-value; PKG, protein kinase G; UALCAN, The University of Alabama at Birmingham Cancer Data Analysis Portal.

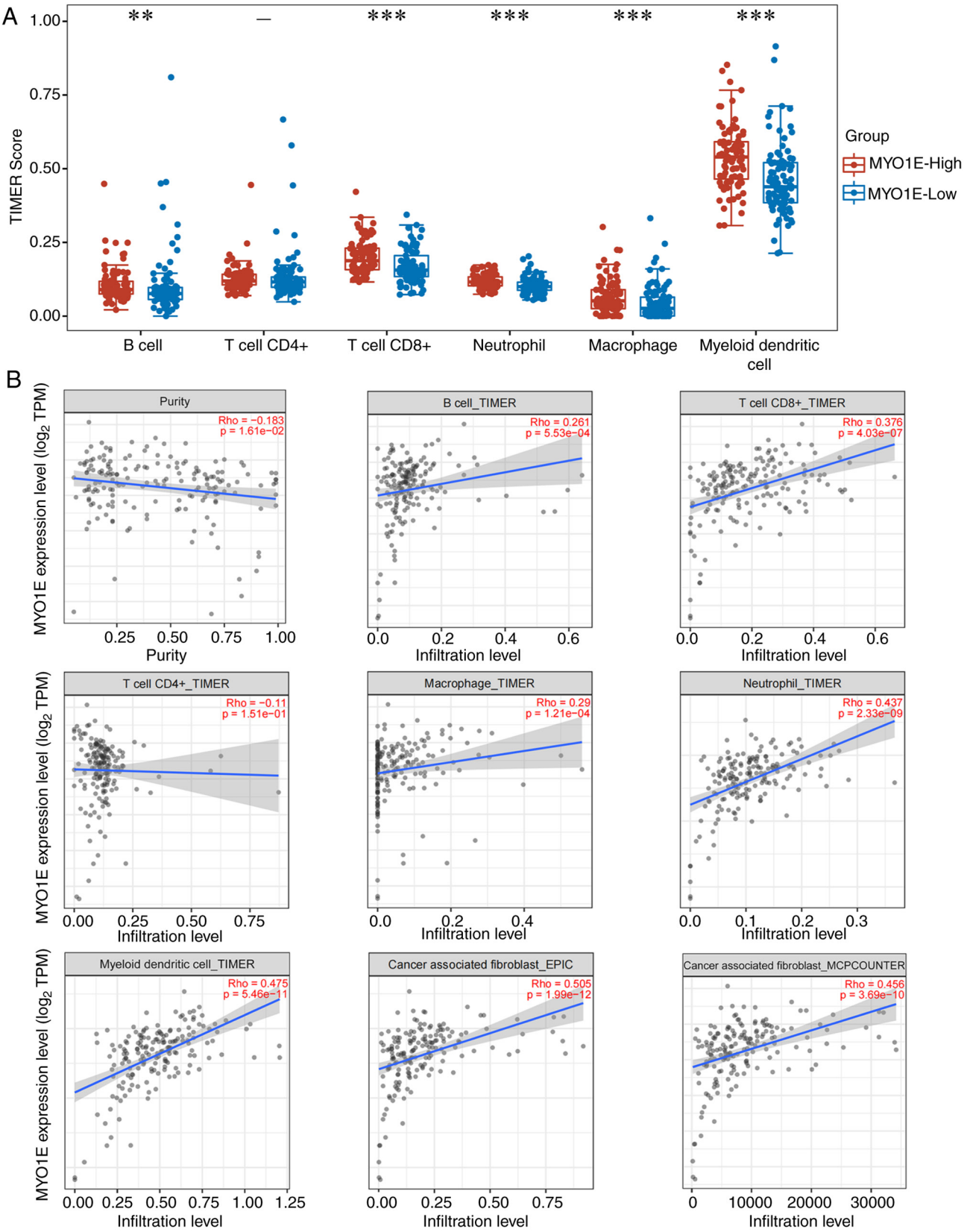

Figure 8. MYO1E is correlated with tumor-infiltrating immune cells. (A) Based on The Cancer Genome Atlas data (version 35), the TIMER algorithm evaluated the relationship between MYO1E and immune infiltrating cells. (B) Exploring the correlation between MYO1E, and immune infiltrating cells and cancer-associated fibroblast infiltration using the TIMER2.0 database. **P<0.01, ***P<0.001. MYO1E, myosin 1E; TIMER, Tumor Immune Estimation Resource; TPM, transcripts per million; EPIC, Estimate the Proportion of Immune and Cancer cells; MCPCOUNTER, Microenvironment Cell Populations-counter.

structural domain, calmodulin-binding neck region, and tail structural domain of F-actin (37). MYO1E has been reported to promote cellular endocytosis, migration, and cell motility in various ways (38,39). This protein's functional abnormalities

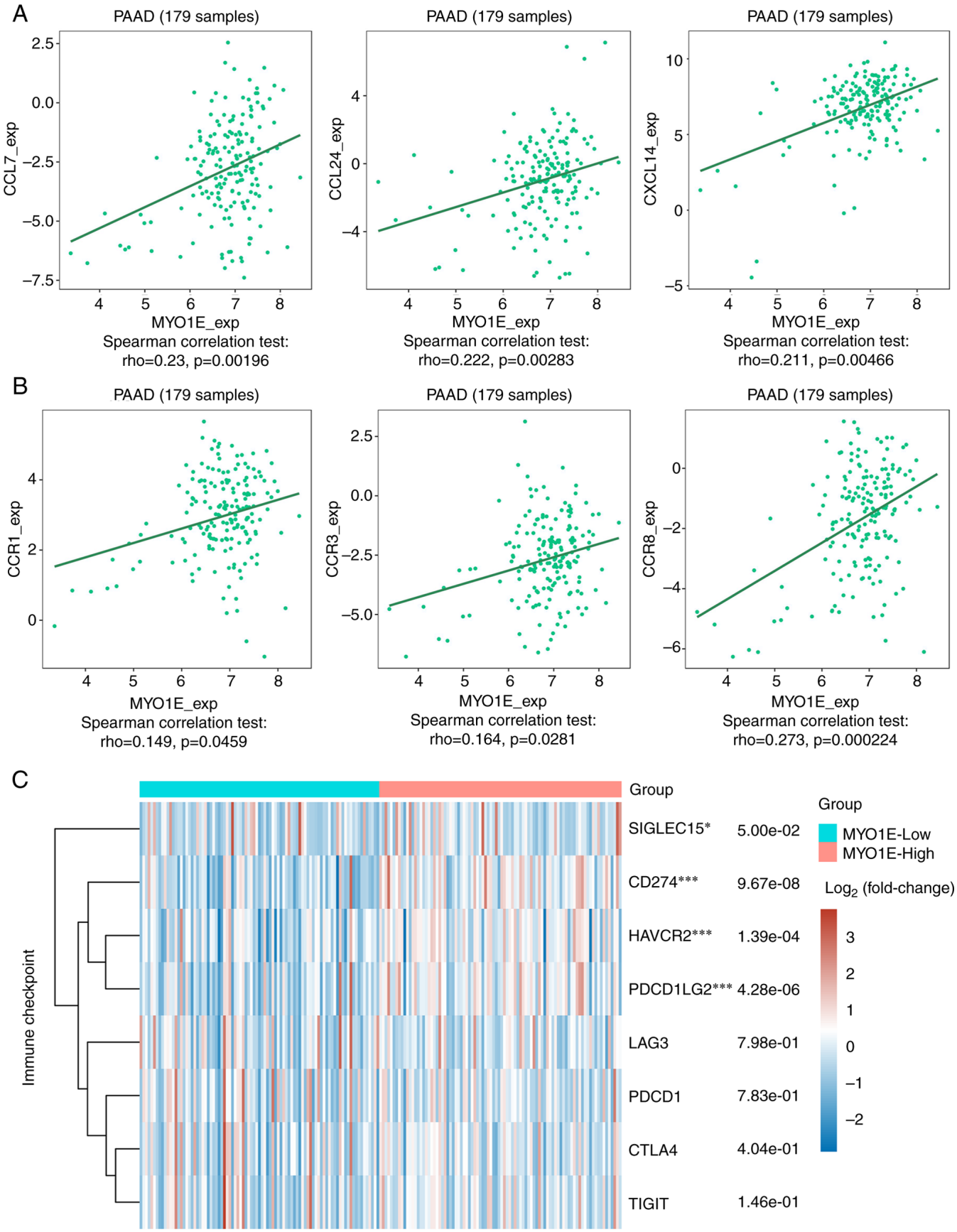

Figure 9. Association of MYO1E expression with chemokines/receptors and immune checkpoints. Scatter plots of MYO1E and (A) CCL7, CCL24, CXCL14, (B) CCR1, CCR3 and CCR8 generated using the TISIDB database. (C) Based on The Cancer Genome Atlas data (version 35), patients were divided into MYO1E high and low expression groups. The expression levels of CD274, CTLA4, HAVCR2, LAG3, PDCD1, PDCD1LG2, TIGIT and SIGLEC15 in the two groups were analyzed using the 'ggplot2' package, and the 'pheatmap' package was used to obtain the expression heat map. *P<0.05, ***P<0.001 (high vs. low expression groups). CCL, C-C motif chemokine ligand; CCR, C-C motif chemokine receptor; CXCL14, C-X-C motif chemokine ligand; MYO1E, myosin 1E; PAAD, pancreatic adenocarcinoma.

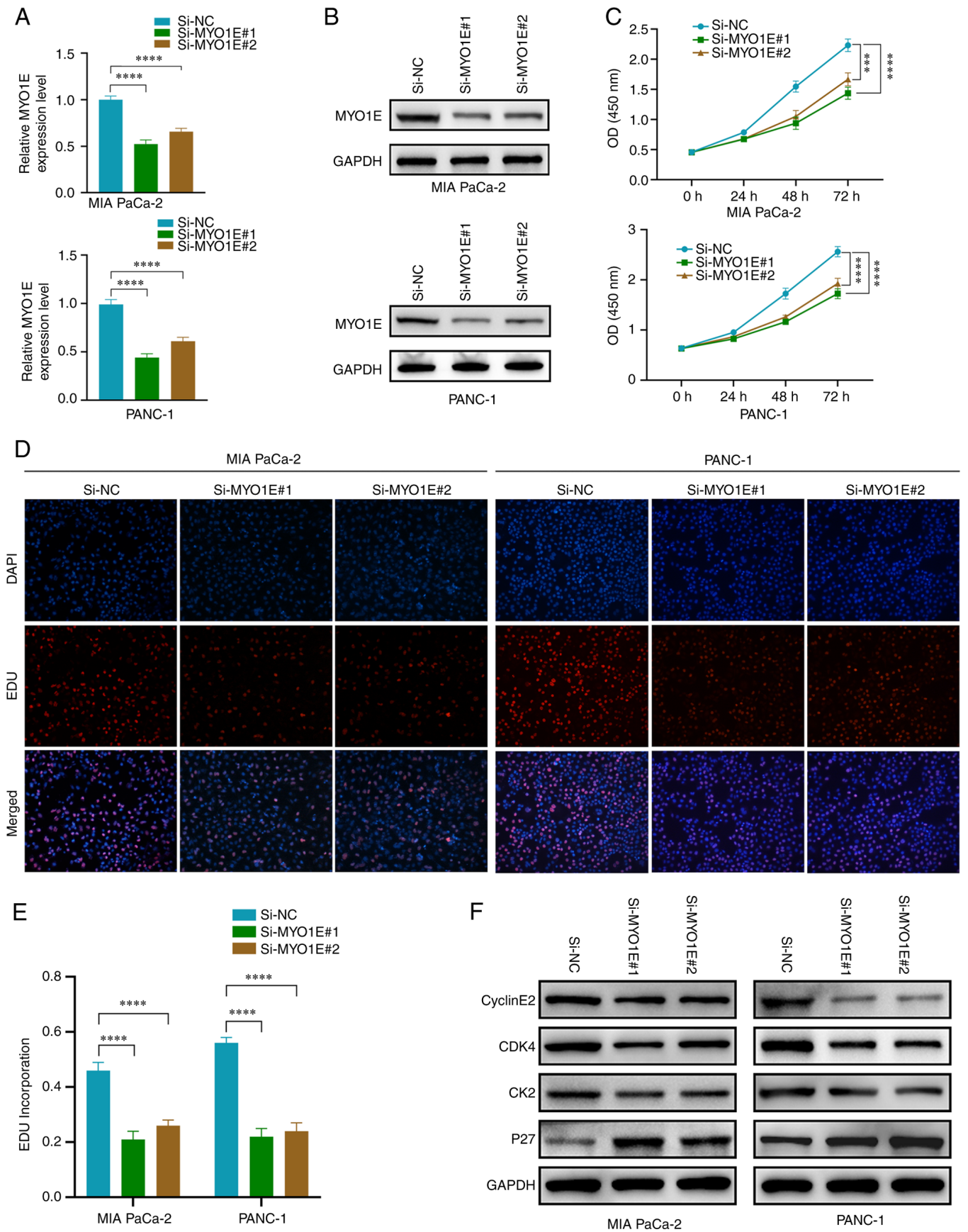

Figure 10. MYO1E silencing reduces the proliferation of PAAD cells. (A) Reverse transcription-quantitative PCR and (B) western blotting were performed to verify the transfection efficiency. (C) Cell Counting Kit-8 assays were performed to examine the effects of MYO1E knockdown on PAAD cell viability. (D) EDU assays were performed to examine the effects of MYO1E knockdown on PAAD cell proliferation. Magnification, x100. (E) Quantitative analysis of PAAD cell proliferation rate. (F) Expression levels of CyclinE2, CDK4, CDK2 and P27 after knockdown of MYO1E. (A, C and E) The least significant difference post hoc test was used. ***P<0.001, ****P<0.0001. EDU, 5-ethynyl-2-deoxyuridine; MYO1E, myosin 1E; NC, negative control; OD, optical density; PAAD, pancreatic adenocarcinoma; Si, small interfering RNA.

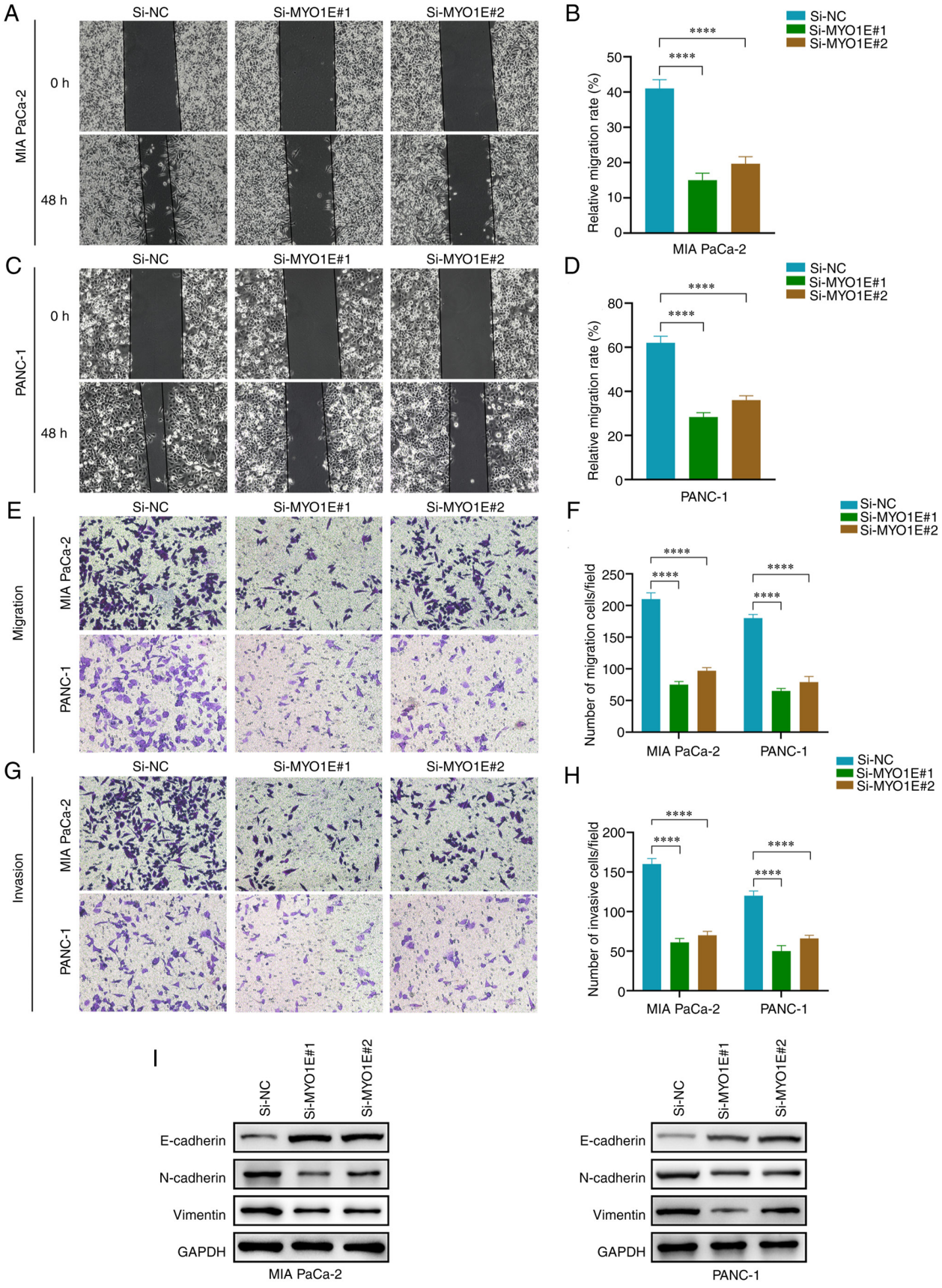

Figure 11. Silencing MYO1E inhibits PAAD cell invasion and migration. (A) Evaluation of MIA PaCa-2 cell migration using a wound-healing experiment (magnification, x100). (B) Quantitative analysis of wound healing rate of MIA PaCa-2 cells. The percentage of the wound healing was calculated as: (width of wound at 0 h-width of wound at 48 h)/width of wound at 0 h. (C) Evaluation of PANC-1 cell migration using a wound-healing experiment (magnification, x100). (D) Quantitative analysis of wound healing rate of PANC-1 cells. (E) Transwell assay of PAAD cell migration (magnification, x100). (F) Quantitative analysis of PAAD cell migration. (G) Transwell assay of PAAD cell invasion (magnification, x100). (H) Quantitative analysis of PAAD cell invasion. (I) Epithelial-mesenchymal transition protein expression after knockdown of MYO1E. (B, D, F and H) The least significant difference post hoc test was used. ****P<0.0001. MYO1E, myosin 1E; NC, negative control; PAAD, pancreatic adenocarcinoma; Si, small interfering RNA.

are found in tumor progression and various pathological states of renal disease (40). Given the limited studies of the MYO1E gene in tumors, we further examined the biological roles and possible regulation mechanisms of MYO1E in PAAD using bioinformatics and *in vitro* functional tests.

We evaluated the mRNA and protein expression levels of MYO1E in several cancer types using TCGA, GTEx, and CPTAC datasets and found that MYO1E was substantially expressed in many tumors. This indicates that MYO1E may have a pro-cancer function in the formation of tumors. The GEO databases revealed that MYO1E expression in PAAD tissues was considerably greater than in normal tissues. We used RT-qPCR and Western blot for validation, and the results were consistent with bioinformatics analysis. In addition, Kaplan-Meier evaluated the predictive significance of MYO1E in PAAD. We found that MYO1E was closely associated with poor OS and poor DFS in PAAD, and MYO1E may function as a PAAD oncogene and prognostic biomarker. We subjected 236 upregulated DEGs to KEGG and GO enrichment analysis and found that upregulated DEGs were linked in the PI3K-Akt-mTOR signaling pathway, ECM-receptor interaction, proteoglycan, and cell-substrate adhesion. We further analyzed MYO1E's potential value in PAAD. We investigated the potential binding protein of MYO1E in PAAD through the PPI protein interaction network. The KEGG and GO enrichment analyses revealed that MYO1E and its interacting proteins were mainly associated with the Ras signaling pathway, phosphatidylinositol signaling system, Hippo signaling pathway, adhesion class, EMT, epithelial cell proliferation, and migration. In addition, we identified two genes, ARPC5 and ARPC2, by cross-tabulation analysis of the dataset. The literature review found that ARPC2 and ARPC5 were involved in migrating invasive tumors (41,42), suggesting that MYO1E may promote PAAD progression through related synergistic effects.

Currently, surgery remains the only radical treatment for patients with PAAD. However, without additional treatment, more than 90% of patients will recur after surgery (43). Immunotherapy, alongside surgery, radiation, and chemotherapy, has been recognized as the fourth pillar of cancer treatment (44). Therefore, we analyzed and studied tumor-infiltrating immune cells, tumor-associated fibroblasts, chemokines, and immune checkpoints in TME. We evaluated the MYO1E score with immune infiltrating cells using the TIMER method and found that high MYO1E expression was positively connected with B cells, $CD8^+$ T cells, neutrophils, macrophages, and dendritic cells in PAAD. Using the MCPCOUNTER and EPIC algorithms, we found that MYO1E is closely related to tumor-associated fibroblasts. Chemokines are crucial for immune cell migration; thus, we analyzed them using by TISIDB database and found that MYO1E was closely associated with CCL7, CCL24, and CXCL14. MYO1E may be involved in migrating immune cells in the TME. Next, we evaluated immune checkpoints and immune checkpoint inhibitors (ICIS), a class of immunotherapies that modulate tumor immune tolerance by blocking specific inhibitory receptor-ligand interactions on the surface of immune cells (45). However, this study was not performed to experimentally validate the role of MYO1E in tumor immunology, which is a limitation of this paper. In the future, we would like to validate the effect of MYO1E on immune cells by flow cytometry and immunohistochemistry experiments. These experiments can further validate the role of MYO1E in tumor immunology. Taken together, MYO1E is implicated in tumor immune modulation and may provide a novel PAAD immunotherapy method. To verify *in vitro* the impact of MYO1E on PAAD cells, we found that suppressing MYO1E decreased the proliferation, invasion, and migration of PAAD cells using CCK-8, EDU, wound healing, Transwell, and Western blot assays.

In this work, we initially revealed the potential functions and possible mechanisms of MYO1E in PAAD through a comprehensive analysis of bioinformatics and *in vitro* Assays, but there are still some shortcomings of this study. First, the MYO1E analysis was derived from tumor databases, and errors existed between databases. Second, although we performed functional *in vitro* trials, *in vivo* experimental confirmation is lacking. Finally, clinical data were not assessed as there was a small clinical sample of PAAD in the database. We will do more research to determine the mechanism of action of MYO1E in PAAD.

In conclusion, we performed a bioinformatics-based investigation of the expression, prognosis, and potential pathways of MYO1E in PAAD. We found that MYO1E may regulate the proliferation and migration of PAAD cells and participate in tumor immunology. *In vitro* experiments showed that silencing MYO1E inhibits PAAD cellular proliferation, invasion, and migration. MYO1E may function as a biomarker for PAAD and provide a new strategy for diagnosing and treating PAAD.

Acknowledgements

Not applicable.

Funding

The present study was supported by the National Natural Science Foundation of China (NSFC; grant nos. 81960431 and 81960535), and Hospital-level Science and Technology Plan Project of Guizhou Cancer Hospital (grant no. YJ2019016).

Availability of data and materials

The datasets used and/or analyzed during the current study are available from the corresponding author on reasonable request.

Authors' contributions

SL, XW and YP were responsible for the conception and design of the experiments. PL, XF, CZ and JH contributed substantially to data acquisition, analysis and interpretation. SL wrote the manuscript, XW participated in the drafting of the manuscript and critically revised important intellectual content. YP and XW approved the final version of the manuscript. SL and YP confirm the authenticity of all the raw data. All authors have read and approved the final manuscript.

Ethics approval and consent to participate

The study was approved by the ethics committee of Affiliated Hospital of Guizhou Medical University and the Affiliated Cancer Hospital of Guizhou Medical University (approval no. 2022-138; Guiyang, China). The patients provided written informed consent for participation.

Patient consent for publication

Not applicable.

Competing interests

The authors declare that they have no competing interests.

References

1. Gao H, Xie R, Huang R, Wang C, Wang Y, Wang D, Liu K, Yang C, Yang Q and Chen L: CIRBP regulates pancreatic cancer cell ferroptosis and growth by directly binding to p53. J Immunol Res 2022: 2527210, 2022.
2. Garg SK and Chari ST: Early detection of pancreatic cancer. Curr Opin Gastroenterol 36: 456-461, 2020.
3. Stanciu S, Ionita-Radu F, Stefani C, Miricescu D, Stanescu S II, Greabu M, Ripszky Totan A and Jinga M: Targeting PI3K/AKT/mTOR signaling pathway in pancreatic cancer: From molecular to clinical aspects. Int J Mol Sci 23: 10132, 2022.
4. Tonini V and Zanni M: Pancreatic cancer in 2021: What you need to know to win. World J Gastroenterol 27: 5851-589, 2021.
5. Hu JX, Zhao CF, Chen WB, Liu QC, Li QW, Lin YY and Gao F: Pancreatic cancer: A review of epidemiology, trend, and risk factors. World J Gastroenterol 27: 4298-321, 2021.
6. Krendel M, Kim SV, Willinger T, Wang T, Kashgarian M, Flavell RA and Mooseker MS: Disruption of myosin 1e promotes podocyte injury. J Am Soc Nephrol 20: 86-94, 2009.
7. Shen H, Bao Y, Feng C, Fu H and Mao J: Overexpression of Myo1e promotes albumin endocytosis by mouse glomerular podocytes mediated by Dynamin. PeerJ 8: e8599, 2020.
8. Krendel M, Osterweil EK and Mooseker MS: Myosin 1E interacts with synaptojanin-1 and dynamin and is involved in endocytosis. FEBS Lett 581: 644-650, 2007.
9. Cheng J, Grassart A and Drubin DG: Myosin 1E coordinates actin assembly and cargo trafficking during clathrin-mediated endocytosis. Mol Biol Cell 23: 2891-2904, 2012.
10. Feeser EA, Ignacio CM, Krendel M and Ostap EM: Myo1e binds anionic phospholipids with high affinity. Biochemistry 49: 9353-9360, 2010.
11. Ouderkirk-Pecone JL, Goreczny GJ, Chase SE, Tatum AH, Turner CE and Krendel M: Myosin 1e promotes breast cancer malignancy by enhancing tumor cell proliferation and stimulating tumor cell de-differentiation. Oncotarget 7: 46419-46432, 2016.
12. Chandran UR, Medvedeva OP, Barmada MM, Blood PD, Chakka A, Luthra S, Ferreira A, Wong KF, Lee AV, Zhang Z, *et al*: TCGA Expedition: A Data Acquisition and Management System for TCGA Data. PLoS One 11: e0165395, 2016.
13. GTEx Consortium: The Genotype-tissue expression (GTEx) project. Nat Genet 45: 580-585, 2013.
14. Tang Z, Kang B, Li C, Chen T and Zhang Z: GEPIA2: An enhanced web server for large-scale expression profiling and interactive analysis. Nucleic Acids Res 47: W556-W560, 2019
15. Bardou P, Mariette J, Escudie F, Djemiel C and Klopp C: Jvenn: An interactive Venn diagram viewer. BMC Bioinformatics 15: 293, 2014.
16. Li T, Fu J, Zeng Z, Cohen D, Li J, Chen Q, Li B and Liu XS: TIMER2.0 for analysis of tumor-infiltrating immune cells. Nucleic Acids Res 48: W509-W514, 2020.
17. Ru B, Wong CN, Tong Y, Zhong JY, Zhong SSW, Wu WC, Chu KC, Wong CY, Lau CY, Chen I, *et al*: TISIDB: An integrated repository portal for tumor-immune system interactions. Bioinformatics 35: 4200-4202, 2019.
18. Livak KJ and Schmittgen TD: Analysis of relative gene expression data using real-time quantitative PCR and the 2(-Delta Delta C(T)) method. Methods 25: 402-408, 2001.
19. Lui JW, Moore SPG, Huang L, Ogomori K, Li Y and Lang D: YAP facilitates melanoma migration through regulation of actin-related protein 2/3 complex subunit 5 (ARPC5). Pigment Cell Melanoma Res 35: 52-65, 2022.
20. Mei P, Tey SK, Wong SWK, Ng TH, Mao X, Yeung CLS, Xu Y, Yu L, Huang Q, Cao P, *et al*: Actin-related protein 2/3 complex subunit 2-enriched extracellular vesicles drive liver cancer metastasis. Hepatol Int 16: 603-613, 2022.
21. Kinoshita T, Nohata N, Watanabe-Takano H, Yoshino H, Hidaka H, Fujimura L, Fuse M, Yamasaki T, Enokida H and Nakagawa M, *et al*: Actin-related protein 2/3 complex subunit 5 (ARPC5) contributes to cell migration and invasion and is directly regulated by tumor-suppressive microRNA-133a in head and neck squamous cell carcinoma. Int J Oncol 40: 1770-1778, 2012.
22. Cheng Z, Wei W, Wu Z, Wang J, Ding X, Sheng Y, Han Y and Wu Q: ARPC2 promotes breast cancer proliferation and metastasis. Oncol Rep 41: 3189-3200, 2019.
23. Zhang J, Liu Y, Yu CJ, Dai F, Xiong J, Li HJ, Wu ZS, Ding R and Wang H: Role of ARPC2 in human gastric cancer. Mediators Inflamm 2017: 5432818, 2017.
24. Huang S, Li D, Zhuang L, Sun L and Wu J: Identification of Arp2/3 complex subunits as prognostic biomarkers for hepatocellular carcinoma. Front Mol Biosci 8: 690151, 2021.
25. Huang S, Sun L, Hou P, Liu K and Wu J: A comprehensively prognostic and immunological analysis of actin-related protein 2/3 complex subunit 5 in pan-cancer and identification in hepatocellular carcinoma. Front Immunol 13: 944898, 2022.
26. Huang S, Dong C, Li D, Xu Y and Wu J: ARPC2: A Pan-Cancer prognostic and immunological biomarker that promotes hepatocellular carcinoma cell proliferation and invasion. Front Cell Dev Biol 10: 896080, 2022.
27. He Z, Gu J, Luan T, Li H, Li C, Chen Z, Luo E, Wang J, Huang Y and Ding M: Comprehensive analyses of a tumor-infiltrating lymphocytes-related gene signature regarding the prognosis and immunologic features for immunotherapy in bladder cancer on the basis of WGCNA. Front Immunol 13: 973974, 2022.
28. Zhang D, He W, Wu C, Tan Y, He Y, Xu B, Chen L, Li Q and Jiang J: Scoring system for tumor-infiltrating lymphocytes and its prognostic value for gastric cancer. Front Immunol 10: 71, 2019.
29. Chen X and Song E: Turning foes to friends: Targeting cancer-associated fibroblasts. Nat Rev Drug Discov 18: 99-115, 2019.
30. Barrett RL and Pure E: Cancer-associated fibroblasts and their influence on tumor immunity and immunotherapy. Elife 9: e57243, 2020.
31. Nagarsheth N, Wicha MS and Zou W: Chemokines in the cancer microenvironment and their relevance in cancer immunotherapy. Nat Rev Immunol 17: 559-572, 2017.
32. Ozga AJ, Chow MT and Luster AD: Chemokines and the immune response to cancer. Immunity 54: 859-874, 2021.
33. Zhang Y and Zheng J: Functions of immune checkpoint molecules beyond immune evasion. Adv Exp Med Biol 1248: 201-226, 2020.
34. Tonini V and Zanni M: Early diagnosis of pancreatic cancer: What strategies to avoid a foretold catastrophe. World J Gastroenterol 28: 4235-4248, 2022.
35. Siegel RL, Miller KD and Jemal A: Cancer statistics, 2020. CA Cancer J Clin 70: 7-30, 2020.
36. El Mezgueldi M, Tang N, Rosenfeld SS and Ostap EM: The kinetic mechanism of Myo1e (human myosin-IC). J Biol Chem 277: 21514-21521, 2002.
37. Mele C, Iatropoulos P, Donadelli R, Calabria A, Maranta R, Cassis P, Buelli S, Tomasoni S, Piras R, Krendel M, *et al*: MYO1E mutations and childhood familial focal segmental glomerulosclerosis. N Engl J Med 365: 295-306, 2011.
38. Jin X, Wang W, Mao J, Shen H, Fu H, Wang X, Gu W, Liu A, Yu H, Shu Q and Du L: Overexpression of Myo1e in mouse podocytes enhances cellular endocytosis, migration, and adhesion. J Cell Biochem 115: 410-419, 2014.
39. Tanimura S, Hashizume J, Arichika N, Watanabe K, Ohyama K, Takeda K and Kohno M: ERK signaling promotes cell motility by inducing the localization of myosin 1E to lamellipodial tips. J Cell Biol 214: 475-489, 2016.
40. Navines-Ferrer A and Martin M: Long-tailed unconventional class I myosins in health and disease. Int J Mol Sci 21: 2555, 2020.

41. Yoon YJ, Han YM, Choi J, Lee YJ, Yun J, Lee SK, Lee CW, Kang JS, Chi SW, Moon JH, *et al*: Benproperine, an ARPC2 inhibitor, suppresses cancer cell migration and tumor metastasis. Biochem Pharmacol 163: 46-59, 2019.
42. Kinoshita T, Nohata N, Watanabe-Takano H, Yoshino H, Hidaka H, Fujimura L, Fuse M, Yamasaki T, Enokida H, Nakagawa M, *et al*: Actin-related protein 2/3 complex subunit 5 (ARPC5) contributes to cell migration and invasion and is directly regulated by tumor-suppressive microRNA-133a in head and neck squamous cell carcinoma. Int J Oncol 40: 1770-1778, 2012.
43. Zhu H, Li T, Du Y and Li M: Pancreatic cancer: Challenges and opportunities. BMC Med 16: 214, 2018.
44. Sunami Y and Kleeff J: Immunotherapy of pancreatic cancer. Prog Mol Biol Transl Sci 164: 189-216, 2019.
45. Jagodinsky JC, Bates AM, Clark PA, Sriramaneni RN, Havighurst TC, Chakravarty I, Nystuen EJ, Kim K, Sondel PM, Jin WJ and Morris ZS: Local TLR4 stimulation augments in situ vaccination induced via local radiation and anti-CTLA-4 checkpoint blockade through induction of CD8 T-cell independent Th1 polarization. J Immunother Cancer 10: e005103, 2022.